

# Cryptotanshinone alleviates polycystic ovary syndrome in rats by regulating the HMGB1/TLR4/NF- $\kappa$ B signaling pathway

YIJIAO YANG<sup>1\*</sup>, LING YANG<sup>1\*</sup>, CAO QI<sup>2\*</sup>, GUOHUA HU<sup>1</sup>,  
LONGHUI WANG<sup>1</sup>, ZHUOJUN SUN<sup>1</sup> and XIAORONG NI<sup>1</sup>

<sup>1</sup>Department of Gynecology, Shanghai University of Traditional Chinese Medicine, Shanghai Traditional Chinese Medicine Hospital, Shanghai 200071; <sup>2</sup>Department of Chinese and Western Medicine, Obstetrics and Gynecology Hospital, Fudan University, Shanghai 200011, P.R. China

Received May 22, 2019; Accepted June 23, 2020

DOI: 10.3892/mmr.2020.11469

**Abstract.** Cryptotanshinone (CRY) has been demonstrated to reverse reproductive disorders. However, whether CRY is effective in the treatment of polycystic ovary syndrome (PCOS) remains unknown. The aim of the present study was to evaluate the therapeutic potential of CRY in PCOS. A rat model of PCOS was established by daily injection of human chorionic gonadotropin and insulin for 22 days. Total body weight and ovarian weight, as well as the levels of luteinizing hormone (LH) and the LH to follicle-stimulating hormone (FSH) ratio (LH/FSH) significantly increased in rats with PCOS, compared with controls. Moreover, the levels of testosterone (T), tumor necrosis factor (TNF)- $\alpha$  and high-mobility group box 1 protein (HMGB1) also increased. However, CRY treatment attenuated the increase in body weight, ovarian weight, LH, LH/FSH ratio, T, TNF- $\alpha$  and HMGB1 levels, compared with the PCOS group. Treatment with CRY also reduced NF- $\kappa$ B/p65, HMGB1 and toll-like receptor (TLR)4 mRNA and protein expression levels in the ovarian tissue and granulosa cells, both *in vitro* and *in vivo*. Thus, CRY significantly mitigated the changes in body weight, ovary weight, hormone levels and inflammatory factor levels observed in rats with PCOS. Thus, CRY protects against PCOS-induced damage of ovarian tissue, possibly through a regulatory pathway involving HMGB1, TLR4 and NF- $\kappa$ B.

## Introduction

Polycystic ovary syndrome (PCOS) is a complex, progressive, refractory gynecological endocrine disease (1) that clinically manifests as hyperandrogenism with menstrual disorders, infertility, obesity and hemorrhoids (2,3). In addition, PCOS is often linked with various complications, including insulin (INS) resistance, endometrial cancer, hypertension, metabolic syndrome and cardiovascular disease (4-6). PCOS is also a concern for patients of childbearing age because the condition not only causes abnormal menstruation, but also ovulatory dysfunction and infertility (7). Therefore, understanding the pathogenesis of PCOS and developing treatment options for patients with PCOS is of great importance (1,8).

Epidemiological surveys from the Netherlands and other countries indicate that the incidence of PCOS in patients of childbearing age is 10-15% and as high as 90% in patients with clinical anovulatory infertility (1,9). Anovulatory sterility caused by PCOS represents a challenge both in the fields of gynecological endocrinology and reproductive healthcare. However, the molecular mechanisms underlying PCOS pathogenesis remain unclear. In addition, several therapeutic options are based on hormones and metformin drugs, with serious side effects and unsatisfactory results (10). A meta-analysis conducted by Li *et al* (11) revealed that metformin might lead to nausea, diarrhea and abdominal cramping in the treatment of PCOS. Moreover, a study from the Cholesterol Treatment Trialists' Collaboration demonstrated that high dose statin caused some adverse effects, such as headaches, muscle pain and myolysis (12).

Cryptotanshinone (CRY) is a monomeric compound derived from tanshinone with antibacterial, anti-inflammatory, antioxidant, antiaging and cooling effects. In Chinese traditional medicine, CRY is believed to have curative effects against angina, coronary heart disease and myocardial injury (13,14). Previous studies suggested that CRY might be used for the treatment of PCOS (15,16). Yu *et al* (15) demonstrated that CRY could improve ovarian morphology and decrease levels of luteinizing hormone (LH), testosterone (T) and androstenedione in PCOS model rats. In addition, Huang *et al* (17) also reported that CRY could reverse androgen excess and ovarian INS resistance (IR) in mice. However, whether CRY

**Correspondence to:** Dr Xiaorong Ni, Department of Gynecology, Shanghai University of Traditional Chinese Medicine, Shanghai Traditional Chinese Medicine Hospital, 274 Middle Zhi Jiang Road, Shanghai 200071, P.R. China  
E-mail: nixr2015@163.com

\*Contributed equally

**Abbreviations:** CRY, cryptotanshinone; PCOS, polycystic ovary syndrome; HCG, human chorionic gonadotropin; INS, insulin; LH, luteinizing hormone; FSH, follicle-stimulating hormone; TNF- $\alpha$ , tumor necrosis factor- $\alpha$ ; HMGB1, high-mobility group box 1

**Key words:** CRY, PCOS, hormone, inflammatory factor, HMGB1, Toll-like receptor 4, nuclear factor- $\kappa$ B

can reverse ovulatory dysfunction caused by PCOS remains unclear.

Our previous study suggested an association between high-mobility group box 1 protein (HMGB1) and IR in PCOS (8). A previous study demonstrated that inhibition of HMGB1 could improve IR in PCOS by suppressing the toll-like receptor (TLR)4/NF- $\kappa$ B signaling pathway (18). Therefore, it was hypothesized that CRY may serve a therapeutic role in PCOS by regulating the HMGB1/TLR4/NF- $\kappa$ B signaling pathway. The aim of the present study was to determine whether CRY can inhibit the reproductive disorders caused by PCOS in a rat model. Moreover, *in vivo* and *in vitro* experiments were carried out in order to evaluate the associations between CRY and HMGB1, as well as the TLR4/NF- $\kappa$ B signaling pathway. The effects of CRY treatment on reproductive hormone levels, ovarian quitiety and inflammatory factors were also assessed. The present findings may provide an experimental basis for future research and clinical applications for ovarian tissue repair.

## Materials and methods

**Animals.** A total of 60 female Sprague-Dawley rats (age, 85 days; weight, 170-200 g) were supplied by Shanghai Laboratory Animal Center, Co. Ltd. The rats were housed at a controlled temperature of  $25\pm 2^{\circ}\text{C}$  in standard cages with  $55\pm 15\%$  humidity and a 12-h dark/light cycle. The animals had free access to water and food. All rats were allowed to acclimatize in their new environment for a period of 7 days before experimentation. All methodological procedures were performed under strict conformity with the guidelines of the Chinese Ministry of Science and Technology for the Care and Use of Laboratory Animals. The experimental protocol was approved by The Animal Care and Experiment Review Board of Shanghai Traditional Chinese Medicine Hospital (Shanghai, China) (approval no. 20190103).

**Reagents.** CRY (>98% purity; cat. no. C5624), INS (cat. no. I9278) and the glucose and sucrose assay kit (cat. no. MAK013) were purchased from Sigma-Aldrich; Merck KGaA. Human chorionic gonadotropin (HCG; cat. no. 161008; Hangzhou Animal Medicine Factory). ELISA kits for LH (cat. no. ab108651), follicle-stimulating hormone (FSH) (cat. no. ab108641), testosterone (cat. no. ab178663) and tumor necrosis factor (TNF)- $\alpha$  (cat. no. ab181421) and the glucose oxidase assay kit (cat. no. ab138884) were purchased from Abcam. Bovine serum albumin (BSA; cat. no. SW3015) and pregnant mare serum gonadotrophin (PMSG; cat. no. P9970) were purchased from Beijing Solarbio Science & Technology Co., Ltd. The EnVision<sup>+</sup> Detection system, (Peroxidase/DAB; rabbit/mouse; cat. no. K406511-2) was purchased from Dako; Agilent Technologies, Inc. Lipofectamine<sup>®</sup> RNAiMAX reagent (cat. no. 13-778-075) was purchased from Invitrogen; Thermo Fisher Scientific, Inc.

**Animal model establishment and drug treatments.** A total of 60 rats were randomly divided into five groups ( $n=12$  in each group): i) Control group, consisting of normal rats receiving an intragastric administration of saline for 3 weeks; ii) PCOS group, consisting of rats with PCOS receiving an intragastric

administration of saline for 3 weeks; iii) PCOS+HMGB1 group, consisting of rats with PCOS intraperitoneally injected with  $80\text{ }\mu\text{g/kg}$  HMGB1 daily and an intragastric administration of saline for 3 weeks; iv) PCOS + CRY group, including rats with PCOS receiving an intragastric administration of CRY for 3 weeks and v) PCOS + HMGB1 + CRY group, including rats with PCOS intraperitoneally injected with  $80\text{ }\mu\text{g/kg}$  HMGB1 daily and an intragastric administration of CRY for 3 weeks. CRY was dissolved in normal saline and administered orally once daily ( $27\text{ mg/kg}$ ) (19).

The rat model of PCOS was established according to the protocol of a previous study (20), with some modifications (the dose of INS used in the present study was lower compared with the the previous study). Briefly, 48 rats were injected subcutaneously with HCG ( $3.0\text{ IU/day}$ ) and INS twice daily for 22 days. INS was increased from  $0.5$  to  $3.0\text{ U/day}$  from day 1 to day 11, and was maintained at  $3.0\text{ U/day}$  until the 22nd day (Table I). The remaining 12 rats (control group) were injected subcutaneously with an equal volume of normal saline twice daily for 22 days. Daily drinking water was replaced with 5% dextrose solution at the beginning of the experiment. All rats were weighed once a week, and a vaginal smear was performed daily until the 23rd day. The loss of rat normal estrous cycle indicated successful establishment of the PCOS model.

**Determination of Lee's index, body mass index (BMI) and ovarian quitiety.** Both Lee's index and BMI were calculated at the end of the experiment. The length of rats was measured from the nose to the anus (21). Lee's index was calculated as  $\text{weight}^{1/3} \times 10^3/\text{length}$ , and the BMI as  $\text{weight}/\text{length}^2$ , where the length is given in cm and the weight in g. In addition, ovarian quitiety was calculated as follows: Ovarian weight/body weight ( $\text{mg}/100\text{ g}$ ).

**Specimen collection.** At the end of the experimental period, rats were fasted overnight then anesthetized with intraperitoneal injection of  $55\text{ mg/kg}$  sodium pentobarbitone. A volume of 5-7 ml blood was then collected from the abdominal aorta and centrifuged at  $1,500 \times g$  for 20 min at  $4^{\circ}\text{C}$  to obtain serum. The rats were sacrificed using  $250\text{ mg/kg}$  pentobarbital sodium and animal death was confirmed by exsanguination. Ovarian tissue was dissected on ice and weighed. For subsequent analysis, one-half of each sample was fixed in 4% paraformaldehyde solution for 24 h at  $25^{\circ}\text{C}$ , while the remaining tissue was stored at  $-80^{\circ}\text{C}$ .

**Determination of LH, LH/FSH ratio, T and TNF- $\alpha$  levels.** The serum levels of LH, T, FSH and TNF- $\alpha$  were determined using ELISA kits, according to the manufacturer's protocol. Absorbance was spectrophotometrically determined at 450 nm.

**Histomorphometry analysis.** Fixed tissues were dehydrated in ascending ethanol concentrations (50, 70, 80 and 90%) for 30 sec and 100% ethanol three times for 30 sec, then washed in xylene. The samples were then embedded in paraffin, and cut to  $4\text{-}\mu\text{m}$  thickness. The sections were subjected to picric acid staining for 30 min at room temperature and hematoxylin-eosin staining for 15 min at room temperature, respectively. Histology and histomorphometry of the stained

Table I. Schedule of INS injection.

Day	INS dose (U/day)
1-2	0.5
3-4	1.0
5-6	1.5
7-8	2.0
9-10	2.5
11-22	3.0
INS, insulin.	

slides were investigated using a Leica DM5000 fluorescence microscope (Leica Microsystems, Inc.; magnification, x100).

**Immunohistochemical analysis.** Ovarian tissue was fixed in 4% paraformaldehyde for 24 h at 4°C, then embedded in paraffin and cut into 4- $\mu$ m thick sections. The sections were then blocked for 30 min at 25°C in a solution of 0.5% BSA, then incubated with anti-HMGB1 antibody (1:200; cat. no. ab227168; Abcam) at 4°C overnight. Subsequently, the sections were incubated with a biotinylated secondary antibody (1:300; cat. no. ab7176; Abcam) for 30 min at 25°C. The visualization of the immune complexes was carried out using the Dako EnVision<sup>+</sup> Detection System kit, according to the manufacturer's protocol. The slides were counterstained using hematoxylin at 25°C for 5 min, then observed under a Leica DM5000 fluorescence microscope (Leica Microsystems, Inc.; magnification, x100) (22).

**Isolation and culture of rat ovarian granulosa cells (GCs).** For the isolation of the GCs, six immature (age, 21-25 days) female rats were administered a subcutaneous injection of PMSG (150 IU/kg), and their ovaries collected after 48 h. The follicular puncture approach (23) was then used to isolate ovarian GCs, which were then pooled. The cells were filtered, then centrifuged at 200 x g for 5 min at 4°C. Following centrifugation, the supernatant was discarded and the GCs were resuspended in Dulbecco's modified Eagle's medium (Thermo Fisher Scientific, Inc.) supplemented with 0.05 mg/ml gentamicin, transferrin, selenium and INS. The isolated GCs were seeded into a 6-well cell culture plate (5x10<sup>4</sup>/ml) and incubated in a 5% CO<sub>2</sub> atmosphere at 37°C in a humidified atmosphere for 24 h.

**Establishment of the IR models of GCs.** To establish IR, the GCs were treated with 1  $\mu$ mol/l dexamethasone for 72 h. The cultured media was harvested for measurement of glucose concentrations using a commercial glucose and sucrose assay kit.

**Cell transfection.** A commercially synthesized HMGB1-specific small interfering (si) RNA (Shanghai GeneChem Co. Ltd.) was used for HMGB1 silencing, together with AllStars scrambled siRNA as the negative control (NC; cat. no. 1027280; Qiagen GmbH). The siRNA sequences were as follows: si-HMGB1#1, 5'-GGACAAGGCCCGTTATGAA-3'; si-HMGB1#2, 5'-UCU

UGACCACAGAUCUAAA-3'; and si-HMGB1#3, 5'-GGCUGACAAGGCUCGUUAU-3'. The resultant siRNA was purified, quantified and suspended in water at a concentration of 0.5  $\mu$ g/ $\mu$ l. siRNA (0.5  $\mu$ l) was combined with 0.5  $\mu$ l Lipofectamine<sup>®</sup> RNAiMAX reagent (50 nM; Thermo Fisher Scientific, Inc.) for 20 min before subsequent experimentation. GCs in the logarithmic growth phase were trypsinized and inoculated into a 6-well cell culture plate (3-5x10<sup>4</sup> cells/ml). When confluence reached 90-95%, GCs were allocated to the following groups: i) Control, untransfected cells; ii) si-NC, cells transfected with plasmid containing non-targeting siRNA; iii) si-HMGB1#1, cells transfected with HMGB1 siRNA-1 recombinant plasmid; iv) si-HMGB1#2, cells transfected with HMGB1 siRNA-2 recombinant plasmid; and v) si-HMGB1#3, cells transfected with HMGB1 siRNA-3 recombinant plasmid. At 24 h post-transfection, transfection efficiency was evaluated by reverse transcription-quantitative (RT-q) PCR and western blot analysis. si-HMGB1#2 displayed the highest silencing efficiency and was therefore used to transfect INS-resistant GCs for further analysis.

**Cell treatment and viability assay.** GCs were divided into five groups: i) Control group, untreated GCs; ii) IR group, INS-resistant GCs; iii) IR + NC group, INS-resistant GCs transfected with si-NC; iv) IR + si-HMGB1, INS-resistant GCs transfected with si-HMGB1; and v) IR + CRY group, INS-resistant GCs treated with 300 nmol/l CRY (17). An MTT assay was used to assess the viability of GCs in each group. Cells were cultured at a seed density of 1x10<sup>4</sup> cells/well in 96-well plates. A final concentration of 0.2 mg/ml MTT reagent (Sigma-Aldrich; Merck KGaA) was added to each well, and the cells were incubated for 4 h at 37°C with 5% CO<sub>2</sub>. DMSO was used to dissolve the formazan crystals for 20 min. Cell viability was calculated after measuring the absorbance at 490 nm with a Safire 2 microplate reader (Tecan Group, Ltd.).

**RNA isolation and RT-qPCR.** TRIzol<sup>®</sup> reagent (cat. no. 10-296-010; Invitrogen; Thermo Fisher Scientific, Inc.) was used for the extraction of total RNA from cells. Total RNA was reverse transcribed into cDNA using the GoScript<sup>™</sup> Reverse Transcription System (Promega Corporation), according to the manufacturer's protocol for 60 min at 42°C. RT-qPCR was performed to determine the mRNA expression levels of HMGB1, TLR4 and NF- $\kappa$ B/p65 using SYBR-Green PCR master mix (Thermo Fisher Scientific, Inc.). The thermocycling conditions used for qPCR were as follows: 50°C UNG activation step; denaturation for 30 sec at 95°C; followed by 40 cycles of denaturation for 5 sec at 95°C and annealing for 30 sec at 60°C. The mRNA expression levels relative to  $\beta$ -actin were obtained using the 2<sup>- $\Delta\Delta$ C<sub>q</sub></sup> method (24). Primer sequences used in the present study are provided in Table II.

**Western blot analysis.** Cells were lysed on ice for 30 min using RIPA protein lysate (cat. no. ab7937; Abcam) and centrifuged at 11,500 x g for 20 min at 4°C. The concentration of total protein in the collected supernatant was measured using a BCA Protein Assay kit (cat. no. 23227; Thermo Fisher Scientific, Inc.). A total of 50  $\mu$ g protein was purified by 12% SDS-PAGE, then transferred onto PVDF membranes.

Table II. Primer sequences for reverse transcription-quantitative PCR.

Gene	Primer sequence, 5'-3'
<i>HMGB1</i>	
Forward	TGAGGGACAAAAGCCACTCC
Reverse	TTGGGAGGGCGGAGAATCA
<i>TLR4</i>	
Forward	TTGGCTTAGAAAACCAAGGTGG
Reverse	ATTGAGCTTCCCGCCTGAAA
<i>NF-<math>\kappa</math>B/p65</i>	
Forward	GGACACCGCAGCCCCATTA
Reverse	CACCCCTTAGTTTCACCGCA
$\beta$ -actin	
Forward	CTAGCCACGAGAGAGCGAAG
Reverse	TGTACATCTGGGCCTACGGA

HMGB1, high-mobility group box 1; TLR4, toll-like receptor 4; NF- $\kappa$ B, nuclear factor- $\kappa$ B.

The membranes were blocked in 8% skimmed milk for 2 h at 25°C, then incubated with primary antibodies specific for GAPDH (1:5,000; cat. no. ab8245; Abcam), HMGB1 (1:1,000; cat. no. ab227168; Abcam), TLR4 (1:1,000; cat. no. ab22048; Abcam) and NF- $\kappa$ B/p65 (1:1,000; cat. no. ab16502; Abcam) overnight at 4°C. The membranes were then washed with Tris-buffered saline containing 0.05% Tween-20 (TBST) and probed with a HRP-conjugated secondary antibody (1:5,000; cat. no. ab7097; Abcam) for 1 h at 25°C. Signals were detected with ECL reagent (cat. no. WBKLS0050; EMD Millipore). Band intensities were measured using ImageJ software (version 1.47; National Institutes of Health).

**Statistical analysis.** All data are presented as the mean  $\pm$  standard deviation of at least three experiments. Multigroup comparisons were analyzed using one-way ANOVA followed by Bonferroni's post hoc test. Statistical analysis was conducted using GraphPad Prism software version 8.0.1 (GraphPad Software, Inc.).  $P < 0.05$  was considered to indicate a statistically significant difference.

## Results

**Effect of CRY treatment on rat body weight, ovarian quotiety, Lee's index and BMI.** Compared with the control group, the body weights of rats in the PCOS group, PCOS + HMGB1 group and PCOS + HMGB1 + CRY group were significantly increased. Notably, total body weight in PCOS + CRY rats was only marginally increased compared with the control group. Moreover, treatment with CRY significantly decreased body weight, compared with rats with PCOS ( $P < 0.0001$ ; Fig. 1A).

Rats in the PCOS and PCOS + HMGB1 groups had significantly heavier ovaries compared with control rats. The ovarian weight for rats in the PCOS + CRY group were significantly decreased compared with the PCOS group ( $P = 0.0193$ ), and were significantly decreased in the PCOS + HMGB1 + CRY

group compared with PCOS + HMGB1 rats ( $P = 0.0052$ ) (Fig. 1B). Additionally, the ovarian quotiety in the PCOS and the PCOS + HMGB1 groups was significantly increased relative to the control group ( $P = 0.0043$  and  $P < 0.0001$ ). However, CRY treatment significantly reduced ovarian quotiety compared with untreated groups (PCOS group,  $P = 0.0086$ ; PCOS + HMGB1 group,  $P < 0.0001$ ; Fig. 1C). Lee's index and BMI were also significantly increased in the PCOS and PCOS + HMGB1 groups compared with controls (PCOS group,  $P = 0.0095$  and  $P = 0.0007$ ; PCOS + HMGB1 group,  $P = 0.0006$  and  $P < 0.0001$ ; Fig. 1D and E). The results indicated that CRY may serve a potential role in the treatment of PCOS, as indicated by alterations in phenotype.

**Effects of CRY on serum levels of hormonal and inflammatory factors in rats with PCOS.** Serum LH, LH/FSH ratio, T and TNF- $\alpha$  concentrations in the PCOS and PCOS + HMGB1 groups were significantly increased compared with the control group. Moreover, LH, LH/FSH ratio, T and TNF- $\alpha$  concentrations of rats in the PCOS + CRY group were significantly decreased compared with the PCOS group ( $P < 0.0001$ ,  $P = 0.0152$ ,  $P = 0.0051$  and  $P = 0.0008$ ). Moreover, LH, LH/FSH ratio, T and TNF- $\alpha$  concentrations of rats in the PCOS + HMGB1 + CRY group were significantly decreased compared with the PCOS + HMGB1 group ( $P < 0.0001$ ,  $P = 0.0334$ ,  $P = 0.0002$  and  $P = 0.0002$ ; Fig. 2). The results suggested that CRY might display a therapeutic effect against PCOS.

**Pathological morphology.** No structural pathological changes were observed in the control group after examination under a light microscope. In particular, the corpora lutea and follicles ( $6 \pm 3$ /field) were in diverse developmental stages (such as primordial follicles, primary follicles and secondary follicles). The tissues were stained with hematoxylin and normal GC layers (6-8 layers) were counted. Structural pathological changes were observed in the PCOS and PCOS + HMGB1 groups. Moreover, compared with the control group, increased numbers ( $13 \pm 5$ /field) of cystic follicles, which were large and filled with fluid, were recorded, and deteriorated GC layers (0-3) were observed in the PCOS and PCOS + HMGB1 groups. In addition, the numbers of corpora lutea in the PCOS and PCOS + HMGB1 groups were reduced, compared with the control group. Following CRY treatment, the pathological morphology of ovaries in the PCOS and PCOS + HMGB1 groups was reversed, increased GC layers (3-5 layers) and decreased cystic follicles ( $7 \pm 2$ /field) were observed, compared with the PCOS and PCOS + HMGB1 groups (Fig. 3). The pathological morphology results indicated that CRY altered the pathological morphology of PCOS.

**Immunohistochemical staining analysis.** The HMGB1 positive ratio in the PCOS and PCOS + HMGB1 groups was significantly increased compared with the control group ( $P = 0.0092$  and  $P = 0.0061$ ). However, following treatment with CRY, the HMGB1 positivity in the PCOS or PCOS + HMGB1 groups was significantly reduced ( $P = 0.0080$  and  $P = 0.0051$ ). Additionally, the HMGB1 positive ratio in the PCOS + CRY group was significantly lower compared with the PCOS + HMGB1 + CRY group ( $P = 0.0381$ ; Fig. 4). The results

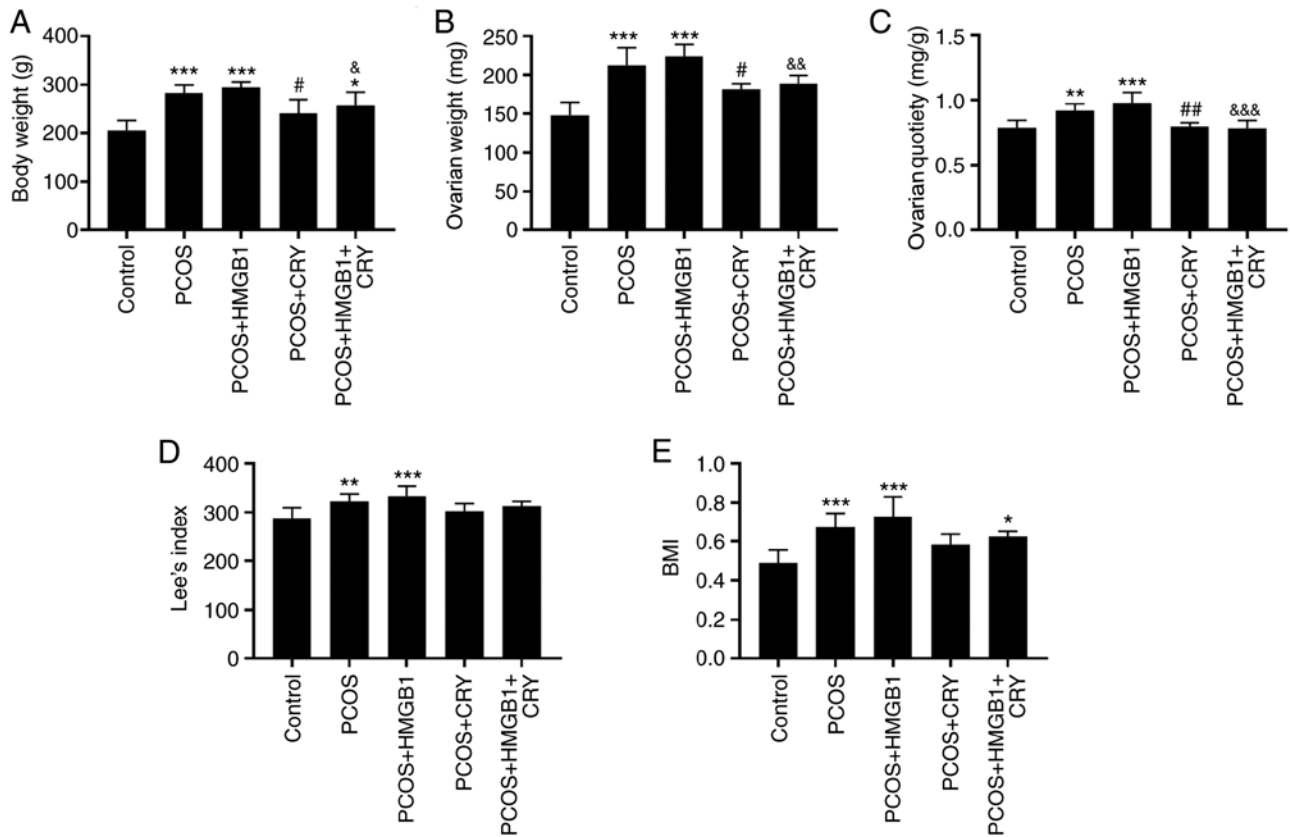


Figure 1. Effects of CRY and HMGB1 on (A) ovarian weight, (B) body weight, (C) ovaries quitiety, (D) Lee's index and (E) BMI in rats with human chorionic gonadotropin and insulin-induced PCOS. Data are presented as the mean  $\pm$  SEM. \* $P < 0.05$ , \*\* $P < 0.01$ , \*\*\* $P < 0.005$  vs. control; # $P < 0.05$ , ## $P < 0.01$  vs. PCOS; & $P < 0.05$ , && $P < 0.01$ , &&& $P < 0.005$  vs. PCOS + HMGB1. CRY, cryptotanshinone; PCOS, polycystic ovary syndrome; HMGB1, high-mobility group box 1; BMI, body mass index.

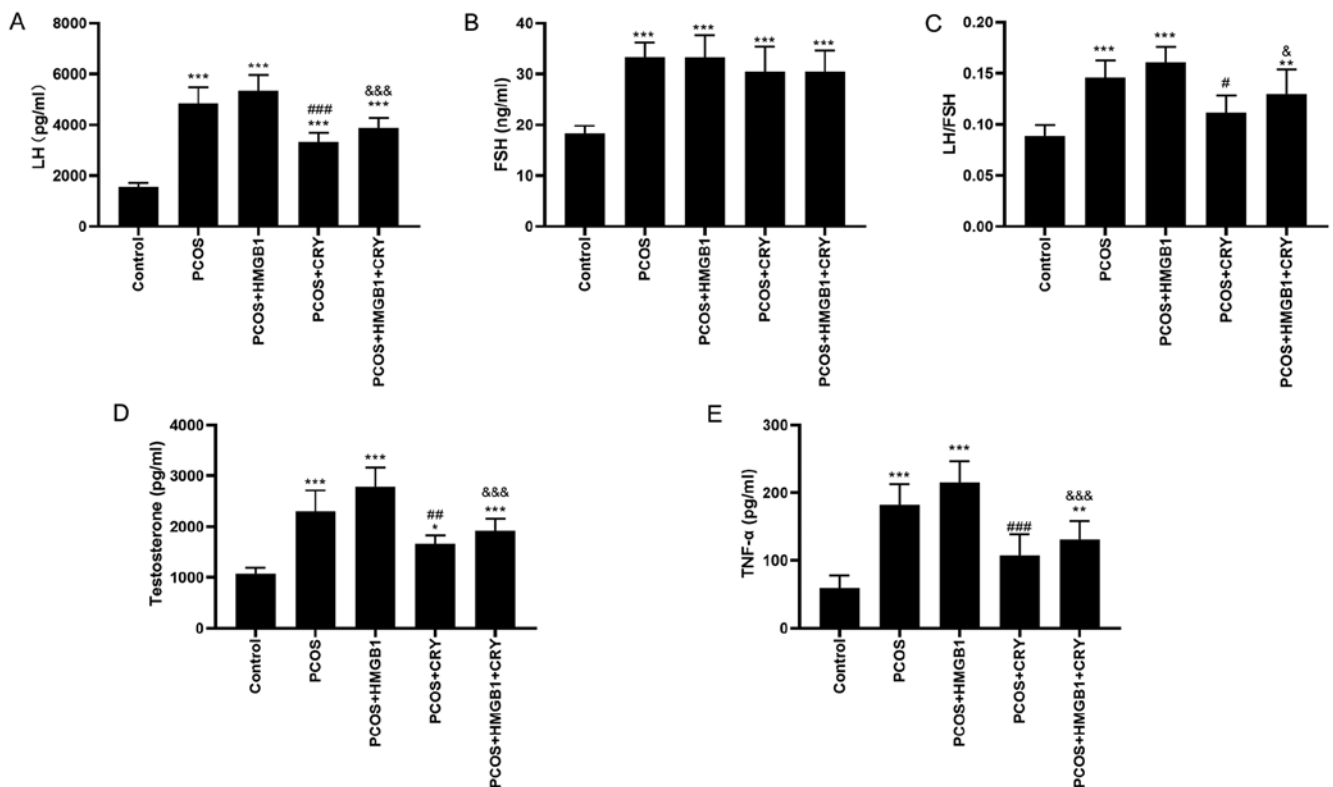


Figure 2. Effect of CRY on serum levels of (A) LH, (B) FSH, (C) LH/FSH ratio, (D) testosterone and (E) TNF- $\alpha$ . Data are presented as the mean  $\pm$  SEM. \* $P < 0.05$ , \*\* $P < 0.01$ , \*\*\* $P < 0.005$  vs. control; # $P < 0.05$ , ## $P < 0.01$ , ### $P < 0.005$  vs. PCOS; & $P < 0.05$ , && $P < 0.01$ , &&& $P < 0.005$  vs. PCOS + HMGB1. CRY, cryptotanshinone; PCOS, polycystic ovary syndrome; LH, luteinizing hormone; FSH, follicle-stimulating hormone; TNF- $\alpha$ , tumor necrosis factor- $\alpha$ ; HMGB1, high-mobility group box 1.



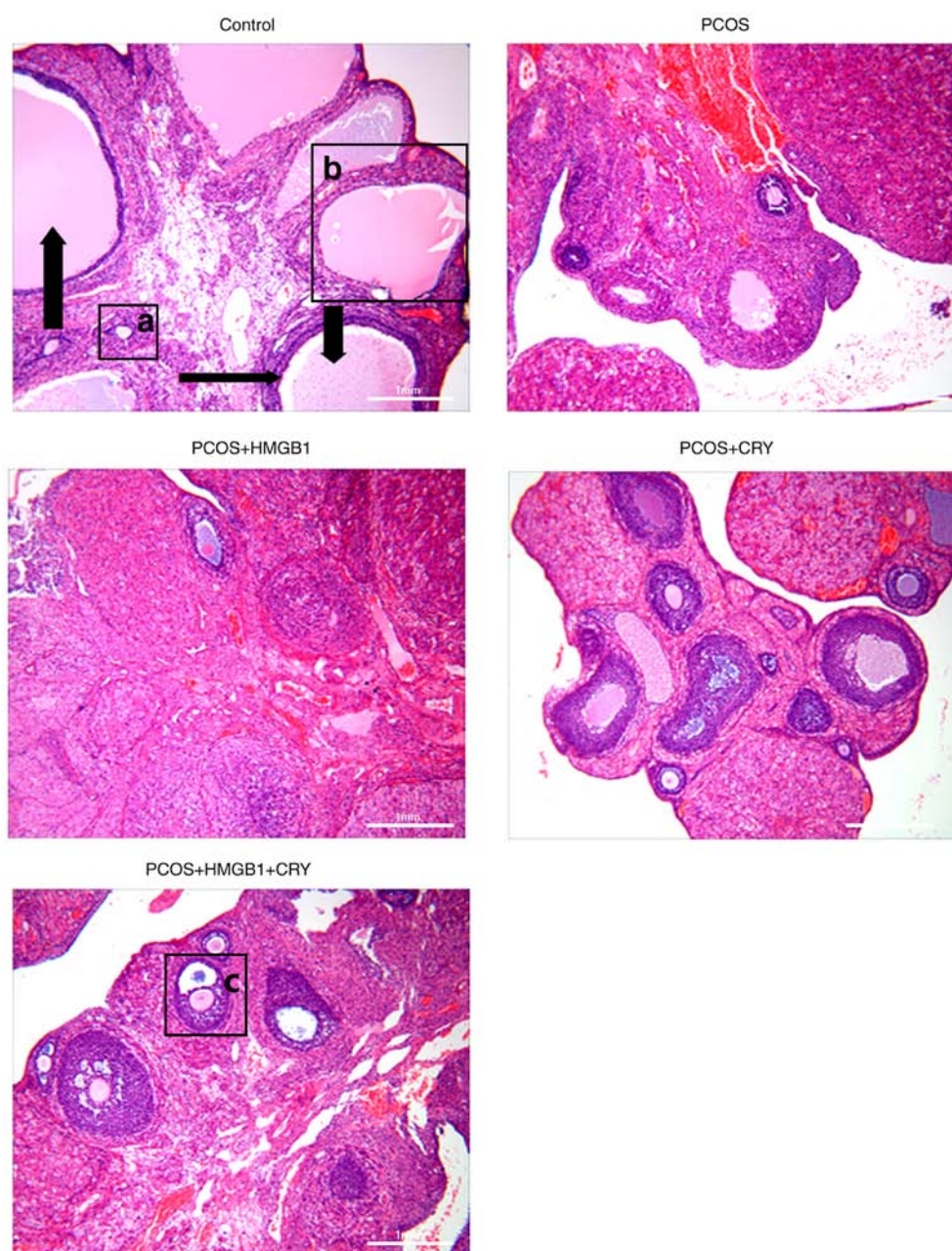


Figure 3. Effects of CRY on pathological morphology of ovarian tissues analyzed under light microscopy. Differences in the numbers of granulosa cell layers (black arrow), cystic follicles (red arrow) and corpora lutea (white arrow) were observed. a: Primordial follicle (a single layer of flattened granulosa cells surrounding the oocyte); b: Primary follicle (a single layer of cuboidal granulosa cells surrounding the oocyte); c: Secondary follicle (two complete layers of cuboidal granulosa cells surrounding the oocyte). Magnification,  $\times 100$ . CRY, cryptotanshinone; PCOS, polycystic ovary syndrome; HMGB1, high-mobility group box 1.

indicated that the therapeutic function of CRY in PCOS might be associated with regulation of HMGB1.

**Effects of CRY on the expression of HMGB1, TLR4 and NF- $\kappa$ B/p65 in the ovarian tissues.** Western blotting and RT-qPCR were used to evaluate the expression levels of HMGB1, TLR4 and NF- $\kappa$ B/p65. Consistent with immunohistochemistry staining, the expressions of HMGB1, TLR4 and NF- $\kappa$ B/p65 in the PCOS and the PCOS + HMGB1 groups significantly increased, compared with the control group (PCOS group:  $P=0.0072$ ,  $P=0.0079$  and  $P=0.0096$ ; PCOS + HMGB1 group:  $P=0.0051$ ,  $P=0.0059$  and  $P=0.0066$ ). Additionally, the expression of these three proteins in the PCOS + HMGB1 + CRY group was significantly lower

compared with the PCOS + HMGB1 group ( $P=0.0067$ ,  $P=0.0073$  and  $P=0.0065$ ), and the expression of these three proteins in the PCOS + CRY group was significantly lower compared with the PCOS group ( $P=0.0058$ ,  $P=0.0063$  and  $P=0.0060$ ). The results suggested that CRY treatment could reduce the expression of HMGB1, TLR4 and NF- $\kappa$ B/p65 in rats with PCOS compared with the PCOS and PCOS + CRY groups. In addition, CRY treatment downregulated the expression of HMGB1, TLR4 and NF- $\kappa$ B/p65 in rats with PCOS and HMGB1 compared with the PCOS + HMGB1 and PCOS + HMGB1 + CRY groups (Fig. 5).

**CRY inhibits proliferation of GCs and regulates TNF- $\alpha$  and HMGB1 expression in vitro.** GCs were transfected with

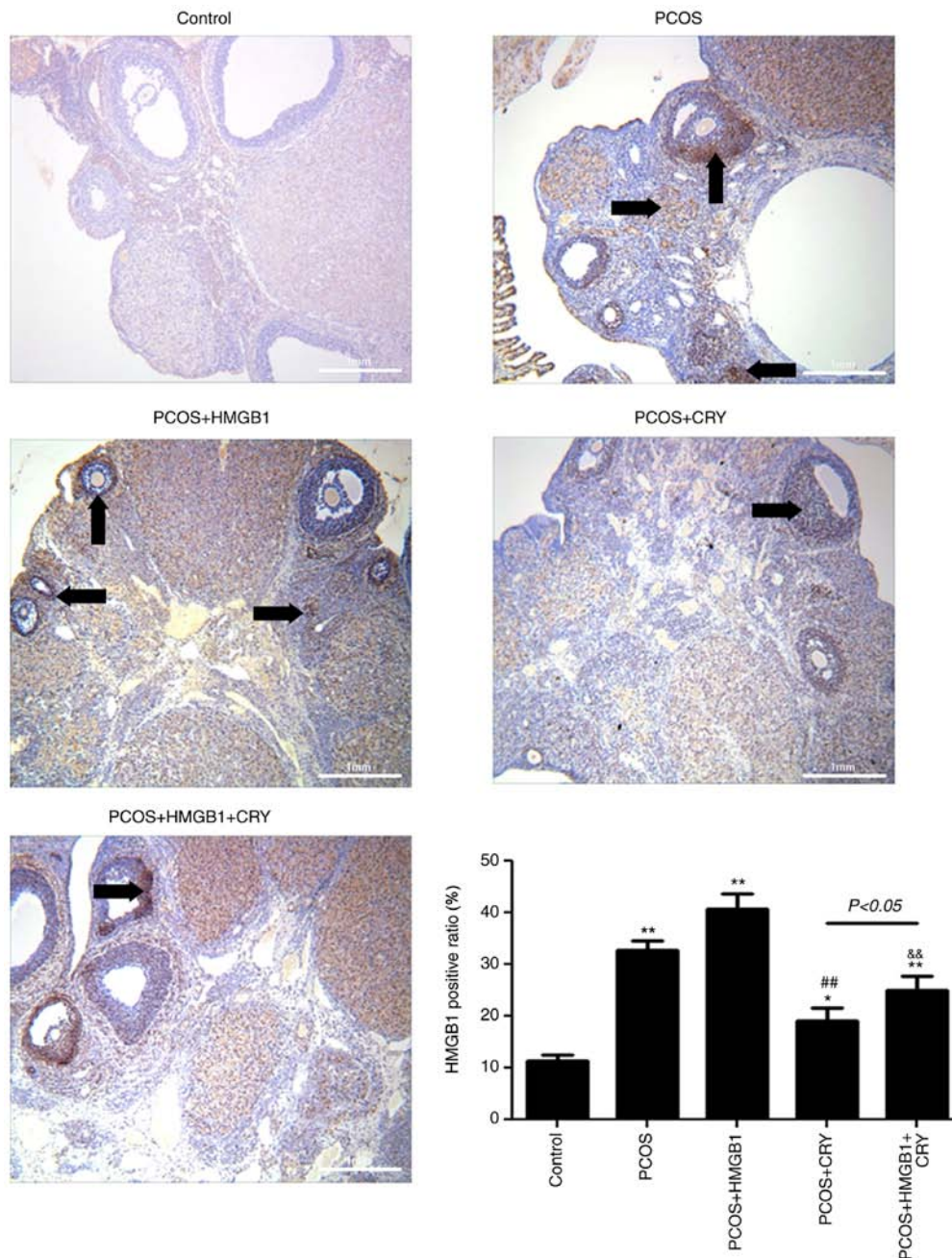


Figure 4. Effects of CRY on HMGB1 expression in ovarian tissues. HMGB1 was primarily expressed in ovarian granulosa cells (black arrow). Magnification, x100. Data are presented as the mean  $\pm$  SEM. \* $P<0.05$ , \*\* $P<0.01$  vs. control; ## $P<0.01$  vs. PCOS; &#& $P<0.001$  vs. PCOS + HMGB1. CRY, cryptotanshinone; PCOS, polycystic ovary syndrome; HMGB1, high-mobility group box 1.

three si-RNAs targeting HMGB1, and HMGB1 mRNA and protein expression levels were evaluated. Compared with si-NC and untransfected cells, mRNA and protein expression of HMGB1 in the si-HMGB1#1, si-HMGB1#2, and si-HMGB1#3 groups was significantly decreased ( $P=0.0061$ ,  $P=0.0031$  and  $P=0.0052$ ), particularly in the si-HMGB1#2 group (Fig. 6A and B). Therefore, the HMGB1 siRNA-2 was used in subsequent experimentation. The viability of GCs in different groups was determined using an MTT assay at 0, 24 and 48 h. Cell viability in the IR and IR + si-NC groups was notably decreased compared with the control group (Fig. 6C). The viability of IR-GCs treated with CRY or transfected with si-HMGB1 was higher compared with untreated cells. In addition, TNF- $\alpha$  and HMGB1 concentrations in the serum of IR

and IR + si-NC rats were significantly increased, compared with the control group ( $P=0.0087$  and  $P=0.0091$ ; Fig. 6D). Moreover, compared with the IR group, TNF- $\alpha$  and HMGB1 concentrations in the IR + si-HMGB1 and IR + CRY groups were significantly reduced ( $P=0.0086$  and  $P=0.0074$ ). The results suggested that CRY improved the viability of IR-GCs by regulating the production of HMGB1.

**Effects of CRY on the expression of HMGB1, TLR4 and NF- $\kappa$ B/p65 in GCs.** HMGB1, TLR4 and NF- $\kappa$ B/p65 expression levels were analyzed using RT-qPCR and western blotting. The expression of HMGB1, TLR4 and NF- $\kappa$ B/p65 in the IR and IR + si-NC groups were significantly increased (IR group,  $P=0.0068$ ,  $P=0.0063$  and  $P=0.0076$ ; IR + si-NC



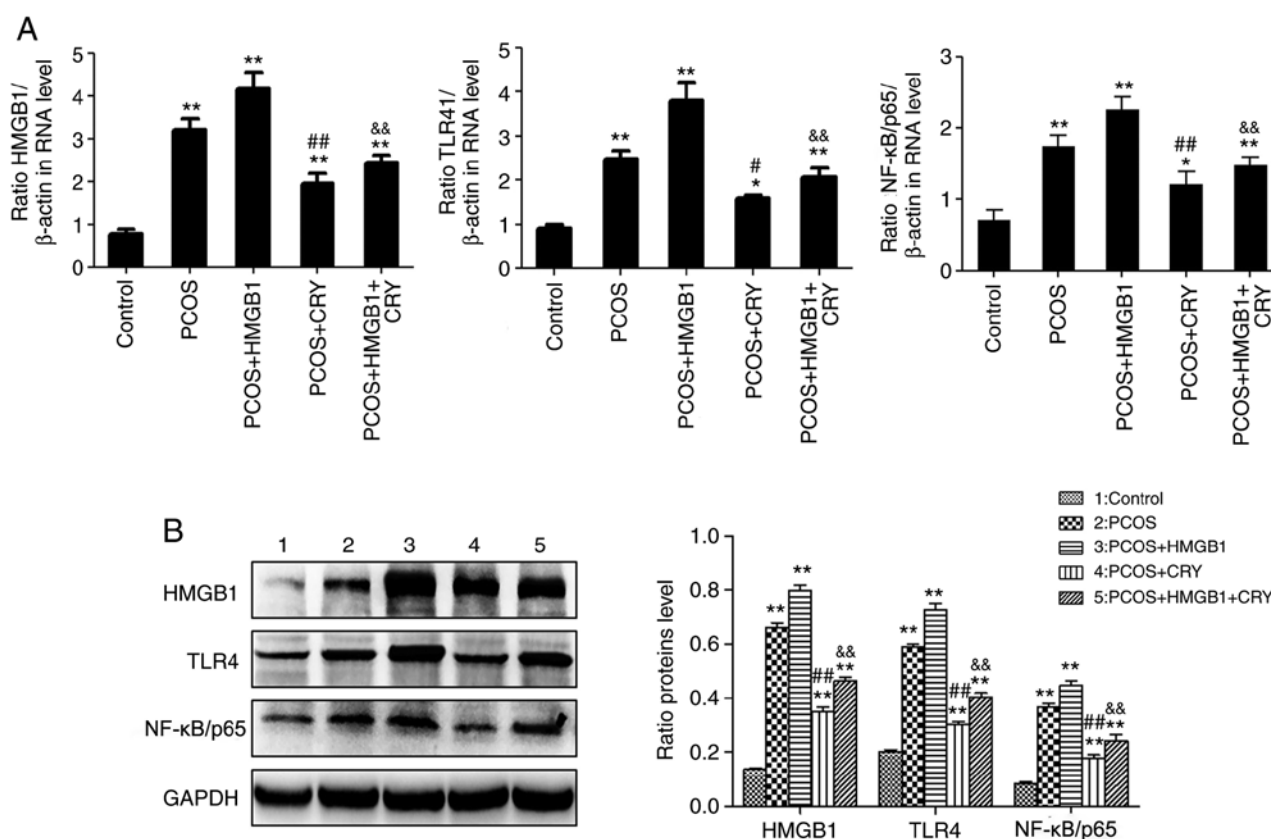


Figure 5. Effects of CRY on HMGB1, TLR4 and NF- $\kappa$ B/p65 expression in ovarian tissues. (A) mRNA expression levels. (B) Protein expression levels. Data are presented as the mean  $\pm$  SEM. \* $P$ <0.05, \*\* $P$ <0.01 vs. control; # $P$ <0.05, ## $P$ <0.01 vs. PCOS; && $P$ <0.001 vs. PCOS + HMGB1. CRY, cryptotanshinone; PCOS, polycystic ovary syndrome; HMGB1, high-mobility group box 1; TLR4, toll-like receptor 4; NF- $\kappa$ B, nuclear factor- $\kappa$ B.

group,  $P=0.0065$ ,  $P=0.0069$  and  $P=0.0079$ ), compared with the control group. Additionally, the expression of HMGB1, TLR4 and NF- $\kappa$ B/p65 in both IR + si-HMGB1 and IR + CRY groups were significantly lower compared with the IR group (IR + si-HMGB group,  $P=0.0098$ ,  $P=0.0093$  and  $P=0.0486$ ; IR + CRY group,  $P=0.0095$ ,  $P=0.0089$  and  $P=0.0339$ ). The effect of CRY treatment on HMGB1, TLR4 and NF- $\kappa$ B/p65 expression levels was also notably greater compared with si-HMGB1 transfection (Fig. 7). The results demonstrated that CRY treatment downregulated the expression of HMGB1, TLR4 and NF- $\kappa$ B/p65.

## Discussion

PCOS is one of the most common endocrinological disorders and is a major cause of anovulatory infertility. PCOS represents a public health concern due to its detrimental effects on women's health and quality of life (25). Thus, there is an urgent need to develop effective therapeutic strategies for patients with PCOS (26,27).

Previous studies have suggested that CRY might be used for the treatment of PCOS (17,28). However, the mechanism through which CRY might reverse ovulatory dysfunction is only partially understood. In our previous study, HMGB1 was upregulated in the peripheral blood of patients with PCOS and INS resistance, and HMGB1 upregulation was correlated with the pathogenesis of PCOS (8). Thus, the aim of the present study was to determine whether CRY could serve a therapeutic

role in PCOS through HMGB1. Several PCOS-related indicators, such as ovarian quitiety, BMI and hormone levels were assessed, suggesting that treatment with HMGB1 could aggravate PCOS, which was consistent with our previous study.

High levels of LH, T and TNF- $\alpha$  are often found in the blood of patients with PCOS, and increased LH/FSH ratio have been reported as a causal factor of PCOS (29,30). In the present study, serum LH, T and TNF- $\alpha$  levels, as well as the LH/FSH ratio were significantly increased in all rats with PCOS, including those treated with HMGB1, compared with the control group. Moreover, CRY treatment decreased the body weight and ovarian quitiety and notably reduced serum LH, LH/FSH ratio, T and TNF- $\alpha$  levels in all PCOS rat groups. These findings suggested that CRY might have a therapeutic effect against PCOS. In addition, pathomorphological analysis further confirmed that CRY could reverse the ovulation disorders seen in PCOS.

Chronic inflammation plays an important role in the development of PCOS (31,32). The TLR4/NF- $\kappa$ B pathway has distinct functions during the stress reaction and inflammation (33). Several studies have demonstrated that HMGB1 could trigger the TLR4 signaling pathway and NF- $\kappa$ B activation, thereby inducing the expression of inflammatory factors (34,35). Jiang *et al* (18) suggested that inhibition of HMGB1 could improve IR in PCOS through the suppression of the TLR4/NF- $\kappa$ B pathway. To determine whether CRY could reverse PCOS by regulating HMGB1/TLR4/NF- $\kappa$ B signaling, the expression of these IR-related markers were evaluated



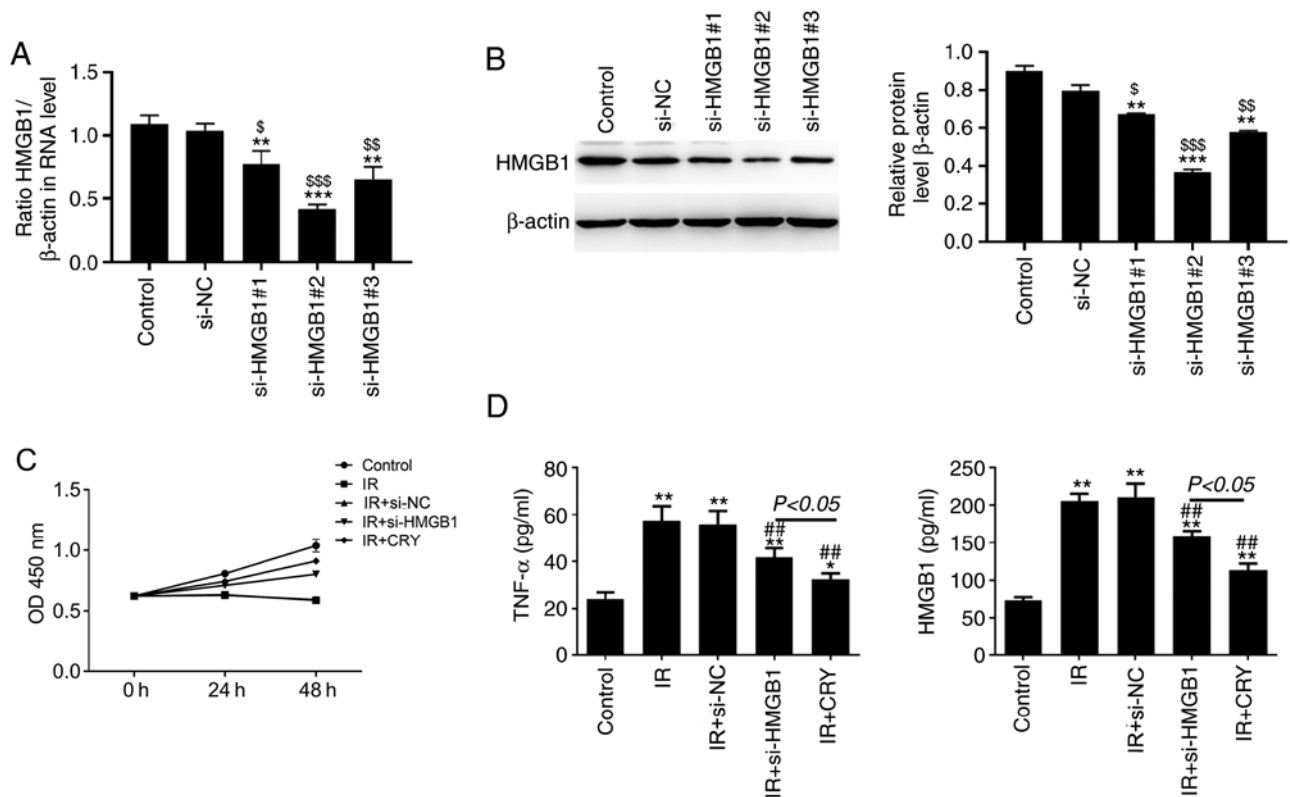


Figure 6. Effect of CRY on GC proliferation, and regulation of TNF- $\alpha$  and HMGB1 expression *in vitro*. (A) mRNA and (B) protein expression of HMGB1 in GCs transfected with siHMGB1. (C) Cell viability of insulin-resistant GCs following CRY treatment or siHMGB1 transfection. (D) Concentration of TNF- $\alpha$  and HMGB1 in culture medium. Data are presented as the mean  $\pm$  SEM. \* $P$ <0.05, \*\* $P$ <0.01, \*\*\* $P$ <0.005 vs. control; <sup>§</sup> $P$ <0.05, <sup>§§</sup> $P$ <0.01, <sup>§§§</sup> $P$ <0.005 vs. si-NC, <sup>##</sup> $P$ <0.01 vs. IR. CRY, cryptotanshinone; IR, insulin resistance; GC, granulosa cell; HMGB1, high-mobility group box 1; TNF- $\alpha$ , tumor necrosis factor- $\alpha$ ; si, small interfering; OD, optical density; si-NC, si-negative control.

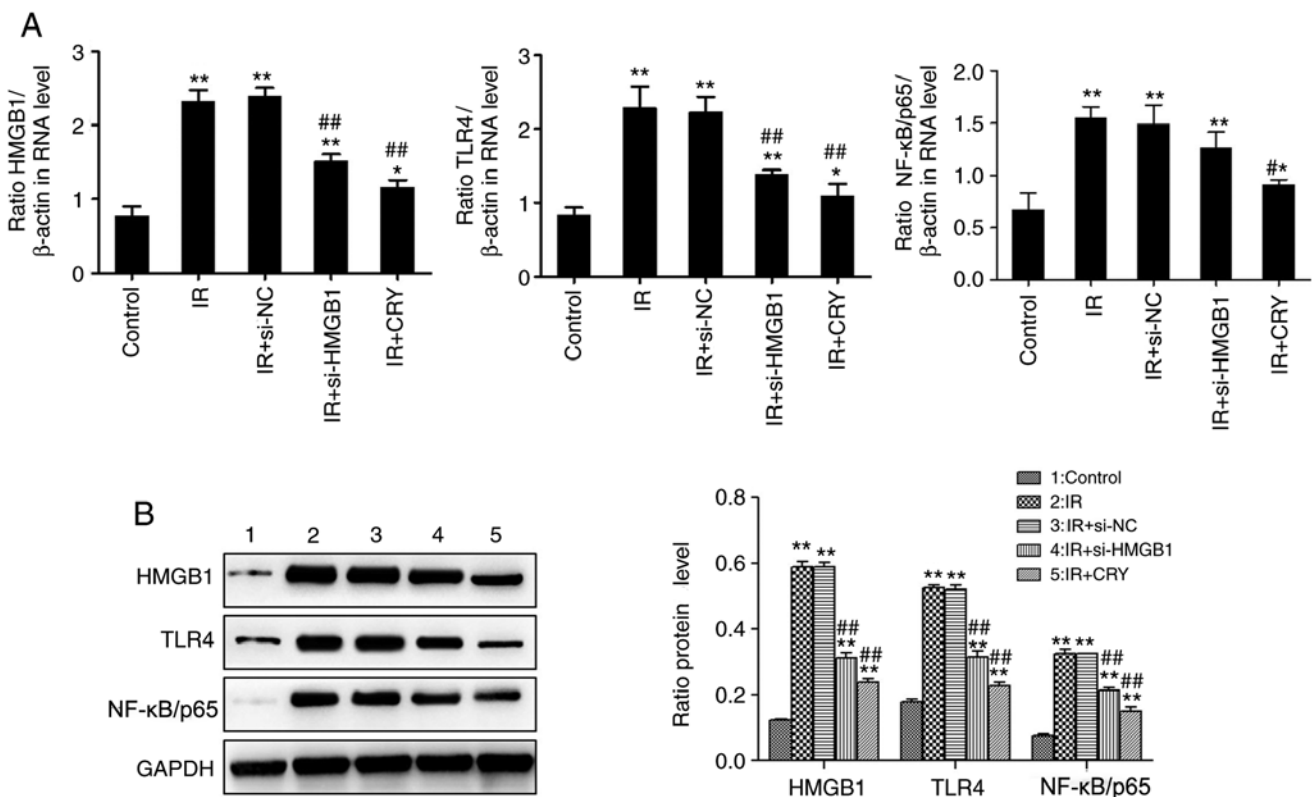


Figure 7. Effects of CRY on HMGB1, TLR4 and NF- $\kappa$ B/p65 expression in ovarian granulosa cells. (A) mRNA expression levels. (B) Protein expression levels. Data are presented as the mean  $\pm$  SEM. \* $P$ <0.05, \*\* $P$ <0.01 vs. control; <sup>§</sup> $P$ <0.05, <sup>§§</sup> $P$ <0.01 vs. IR. CRY, cryptotanshinone; IR, insulin resistance; HMGB1, high-mobility group box 1; TLR4, toll-like receptor 4; NF- $\kappa$ B, nuclear factor- $\kappa$ B; si, small interfering; si-NC, si-negative control.

in ovarian tissue and GCs. HMGB1, TLR4 and NF- $\kappa$ B/p65 expression was upregulated in the ovarian tissue from rats with PCOS, including those treated with HMGB1, consistent with a study conducted by Koc *et al* (36). In contrast, CRY treatment resulted in HMGB1, TLR4 and NF- $\kappa$ B/p65 downregulation, compared with PCOS model rats.

Furthermore, si-HMGB1 silencing experiments were carried out in INS-resistant GCs in order to evaluate the effect of HMGB1 on cell viability and expression of IR-related markers in rats with PCOS. In the present study, immature rats were selected for the isolation of GCs. Compared with GCs from mature rats, the GCs in immature rats had not been exposed to endogenous gonadotropins. Therefore, a large number of GCs could be obtained in the same stage after inducing estrus of immature rats by PMSG. Both transfection with si-HMGB1 and CRY treatment resulted in improved viability in INS-resistant GCs. Several studies have suggested that HMGB1 could promote apoptosis of GCs (36,37). Another previous study demonstrated that HMGB1 silencing significantly reduced GC apoptosis (8). Moreover, in the present study, the concentration of HMGB1 was measured in the GC culture supernatant significantly decreased following CRY and si-HMGB1 treatment, compared with untreated or untransfected cells, further confirming that the protective effects of CRY might be mediated by regulating HMGB1. Furthermore, the results of RT-qPCR and western blotting in INS-resistant GCs were consistent with those in ovarian tissues, suggesting that CRY treatment could reduce the expression of HMGB1, TLR4 and NF- $\kappa$ B/p65 in both PCOS model and INS-resistant GCs.

Collectively, the present findings suggest that CRY might attenuate PCOS, at least in part, by decreasing the serum levels of LH, LH/FSH ratio, T and TNF- $\alpha$  through HMGB1, TLR4 and NF- $\kappa$ B/p65 downregulation in ovarian tissue. However, the current study presents some limitations. Although CRY can decrease the expression of HMGB1, TLR4 and NF- $\kappa$ B/p65 in ovarian tissues from rats with PCOS, the underlying mechanism remains unclear. Moreover, the protective effects of CRY on IR-GCs were not confirmed through validations experiments other than cell viability detection. In summary, the present study demonstrated that CRY treatment may effectively improve PCOS by lowering the serum LH, LH/FSH ratio, T and TNF- $\alpha$  levels and decreasing the expression of HMGB1, TLR4 and NF- $\kappa$ B/p65 in ovarian tissues and GCs. Thus, CRY could represent a potential treatment option for PCOS. Nevertheless, further studies and clinical trials are required to confirm the efficacy and safety of this approach. Furthermore, the present study also provided a novel theoretical basis for the treatment of PCOS through HMGB1, TLR4 and NF- $\kappa$ B/p65.

## Acknowledgements

Not applicable.

## Funding

This work was supported by The National Natural Science Foundation (grant no. 81804136), The Shanghai Natural Science Foundation (grant no. 17ZR1427900) and The Shanghai Municipal Commission Foundation of Health and Family Planning (grant no. 201540087).

## Availability of data and materials

All data generated or analyzed during this study are included in this published article.

## Authors' contributions

GH, LW, ZS, CQ, LY and YY performed the experiments and analyzed data. YY, CQ and LY drafted and revised the manuscript. XN designed the study. All authors read and approved the final manuscript.

## Ethics approval and consent to participate

All methodological procedures were performed under strict conformity with the guidelines of the Chinese Ministry of Science and Technology for the Care and Use of Laboratory Animals. The experimental protocol was approved by The Animal Care and Experiment Review Board of Shanghai Traditional Chinese Medicine Hospital (Shanghai, China) (approval no. 20190103).

## Patient consent for publication

Not applicable.

## Competing interests

The authors declare that they have no competing interests.

## References

1. Witchel SF, Recabarren SE, González F, Diamanti-Kandarakis E, Cheang KI, Duleba AJ, Legro RS, Homburg R, Pasquali R, Lobo RA, *et al*: Emerging concepts about prenatal genesis, aberrant metabolism and treatment paradigms in polycystic ovary syndrome. *Endocrine* 42: 526-534, 2012.
2. Rojas J, Chávez M, Olivar L, Rojas M, Morillo J, Mejías J, Calvo M and Bermúdez V: Polycystic ovary syndrome, insulin resistance, and obesity: Navigating the pathophysiological labyrinth. *Int J Reprod Med* 2014: 719050, 2014.
3. Fauser BC, Tarlatzis BC, Rebar RW, Legro RS, Balen AH, Lobo R, Carmina E, Chang J, Yildiz BO, Laven JS, *et al*: Consensus on women's health aspects of polycystic ovary syndrome (PCOS): The amsterdam ESHRE/ASRM-sponsored 3rd PCOS consensus workshop group. *Fertil Steril* 97: 28-38.e25, 2012.
4. Yuan H, Zhu G, Wang F, Wang X, Guo H and Shen M: Interaction between common variants of FTO and MC4R is associated with risk of PCOS. *Reprod Biol Endocrinol* 13: 55, 2015.
5. Goodarzi MO, Dumesic DA, Chazenbalk G and Azziz R: Polycystic ovary syndrome: Etiology, pathogenesis and diagnosis. *Nat Rev Endocrinol* 7: 219-231, 2011.
6. Ollila MM, Piltonen T, Puukka K, Ruokonen A, Järvelin MR, Tapanainen JS, Franks S and Morin-Papunen L: Weight gain and dyslipidemia in early adulthood associate with polycystic ovary syndrome: Prospective cohort study. *J Clin Endocrinol Metab* 101: 739-747, 2016.
7. Diamanti-Kandarakis E: Polycystic ovarian syndrome: Pathophysiology, molecular aspects and clinical implications. *Expert Rev Mol Med* 10: e3, 2008.
8. Ni XR, Sun ZJ, Hu GH and Wang RH: High concentration of insulin promotes apoptosis of primary cultured rat ovarian granulosa cells via its increase in extracellular HMGB1. *Reprod Sci* 22: 271-277, 2015.
9. Velásquez E: Chronic complications of polycystic ovary syndrome. Review. *Invest Clin* 43: 205-213, 2002 (In Spanish).
10. Huang Y, Sun J, Wang X, Tao X, Wang H and Tan W: Asymptomatic chronic gastritis decreases metformin tolerance in patients with type 2 diabetes. *J Clin Pharm Ther* 40: 461-465, 2015.

11. Li XJ, Yu YX, Liu CQ, Zhang W, Zhang HJ, Yan B, Wang LY, Yang SY and Zhang SH: Metformin vs. thiazolidinediones for treatment of clinical, hormonal and metabolic characteristics of polycystic ovary syndrome: A meta-analysis. *Clin Endocrinol (Oxf)* 74: 332-339, 2011.
12. Cholesterol Treatment Trialists' (CTT) Collaboration; Baigent C, Blackwell L, Emberson J, Holland LE, Reith C, Bhala N, Peto R, Barnes EH, Keech A, *et al*: Efficacy and safety of more intensive lowering of LDL cholesterol: A meta-analysis of data from 170,000 participants in 26 randomised trials. *Lancet* 376: 1670-1681, 2010.
13. Ji XY, Tan BK and Zhu YZ: *Salvia miltiorrhiza* and ischemic diseases. *Acta Pharmacol Sin* 21: 1089-1094, 2000.
14. Wang X, Morris-Natschke SL and Lee KH: New developments in the chemistry and biology of the bioactive constituents of Tanshen. *Med Res Rev* 27: 133-148, 2007.
15. Yu J, Zhai D, Hao L, Zhang D, Bai L, Cai Z and Yu C: Cryptotanshinone reverses reproductive and metabolic disturbances in PCOS model rats via regulating the expression of CYP17 and AR. *Evid Based Complement Alternat Med* 2014: 670743, 2014.
16. Ong M, Peng J, Jin X and Qu X: Chinese herbal medicine for the optimal management of polycystic ovary syndrome. *Am J Chin Med* 45: 405-422, 2017.
17. Huang Y, Li W, Wang CC, Wu X and Zheng J: Cryptotanshinone reverses ovarian insulin resistance in mice through activation of insulin signaling and the regulation of glucose transporters and hormone synthesizing enzymes. *Fertil Steril* 102: 589-596.e584, 2014.
18. Jiang B, Xue M, Xu D, Song Y and Zhu S: Upregulation of microRNA-204 improves insulin resistance of polycystic ovarian syndrome via inhibition of HMGB1 and the inactivation of the TLR4/NF- $\kappa$ B pathway. *Cell Cycle* 19: 697-710, 2020.
19. Yang X, Zhang Y, Wu X, Bae CS, Hou L, Kuang H, Wang Y and Stener-Victorin E: Cryptotanshinone reverses reproductive and metabolic disturbances in prenatally androgenized rats via regulation of ovarian signaling mechanisms and androgen synthesis. *Am J Physiol Regul Integr Comp Physiol* 300: R869-R875, 2011.
20. Poretsky L, Clemons J and Bogovich K: Hyperinsulinemia and human chorionic gonadotropin synergistically promote the growth of ovarian follicular cysts in rats. *Metabolism* 41: 903-910, 1992.
21. Ngo HT, Hetland RB, Sabaredzovic A, Haug LS and Steffensen IL: In utero exposure to perfluorooctanoate (PFOA) or perfluorooctane sulfonate (PFOS) did not increase body weight or intestinal tumorigenesis in multiple intestinal neoplasia (Min/+) mice. *Environ Res* 132: 251-263, 2014.
22. Mangano C, Scarano A, Perrotti V, Iezzi G and Piattelli A: Maxillary sinus augmentation with a porous synthetic hydroxyapatite and bovine-derived hydroxyapatite: A comparative clinical and histologic study. *Int J Oral Maxillofac Implants* 22: 980-986, 2007.
23. deMoura MD, Chamoun D, Resnick CE and Adashi EY: Insulin-like growth factor (IGF)-I stimulates IGF-I and type 1 IGF receptor expression in cultured rat granulosa cells: Autocrine regulation of the intrafollicular IGF-I system. *Endocrine* 13: 103-110, 2000.
24. Livak KJ and Schmittgen TD: Analysis of relative gene expression data using real-time quantitative PCR and the 2(-Delta Delta C(T)) method. *Methods* 25: 402-408, 2001.
25. March WA, Moore VM, Willson KJ, Phillips DIW, Norman RJ and Davies MJ: The prevalence of polycystic ovary syndrome in a community sample assessed under contrasting diagnostic criteria. *Hum Reprod* 25: 544-551, 2010.
26. Azziz R, Marin C, Hoq L, Badamgarav E and Song P: Health care-related economic burden of the polycystic ovary syndrome during the reproductive life span. *J Clin Endocrinol Metab* 90: 4650-4658, 2005.
27. Barthelmeß EK and Naz RK: Polycystic ovary syndrome: Current status and future perspective. *Front Biosci (Elite Ed)* 6: 104-119, 2014.
28. Xia Y, Zhao P, Huang H, Xie Y, Lu R and Li D: Cryptotanshinone reverses reproductive disturbances in rats with dehydroepiandrosterone-induced polycystic ovary syndrome. *Am J Transl Res* 9: 2447-2456, 2017.
29. Rosenfield RL and Ehrmann DA: The pathogenesis of polycystic ovary syndrome (PCOS): The hypothesis of PCOS as functional ovarian hyperandrogenism revisited. *Endocr Rev* 37: 467-520, 2016.
30. Nestler JE, Powers LP, Matt DW, Steingold KA, Plymate SR, Rittmaster RS, Clore JN and Blackard WG: A direct effect of hyperinsulinemia on serum sex hormone-binding globulin levels in obese women with the polycystic ovary syndrome. *J Clin Endocrinol Metab* 72: 83-89, 1991.
31. Shorakae S, Ranasinha S, Abell S, Lambert G, Lambert E, de Courten B and Teede H: Inter-related effects of insulin resistance, hyperandrogenism, sympathetic dysfunction and chronic inflammation in PCOS. *Clin Endocrinol (Oxf)* 89: 628-633, 2018.
32. Liu M, Gao J, Zhang Y, Li P, Wang H, Ren X and Li C: Serum levels of TSP-1, NF- $\kappa$ B and TGF- $\beta$ 1 in polycystic ovarian syndrome (PCOS) patients in northern China suggest PCOS is associated with chronic inflammation. *Clin Endocrinol (Oxf)* 83: 913-922, 2015.
33. Zhang X, Xue C, Xu Q, Zhang Y, Li H, Li F, Liu Y and Guo C: Caprylic acid suppresses inflammation via TLR4/NF- $\kappa$ B signaling and improves atherosclerosis in ApoE-deficient mice. *Nutr Metab (Lond)* 16: 40, 2019.
34. Li G, Wu X, Yang L, He Y, Liu Y, Jin X and Yuan H: TLR4-mediated NF- $\kappa$ B signaling pathway mediates HMGB1-induced pancreatic injury in mice with severe acute pancreatitis. *Int J Mol Med* 37: 99-107, 2016.
35. Osuka K, Watanabe Y, Usuda N, Iwami K, Miyachi S and Takayasu M: Expression of high mobility group B1 and toll-like receptor-nuclear factor  $\kappa$ B signaling pathway in chronic subdural hematomas. *PLoS One* 15: e0233643, 2020.
36. Koc O, Ozdemirici S, Acet M, Soyuturk U and Aydin S: Nuclear factor- $\kappa$ B expression in the endometrium of normal and overweight women with polycystic ovary syndrome. *J Obstet Gynaecol* 37: 924-930, 2017.
37. Kim SW, Lim CM, Kim JB, Shin JH, Lee S, Lee M and Lee JK: Extracellular HMGB1 released by NMDA treatment confers neuronal apoptosis via RAGE-p38 MAPK/ERK signaling pathway. *Neurotox Res* 20: 159-169, 2011.



This work is licensed under a Creative Commons Attribution-NonCommercial-NoDerivatives 4.0 International (CC BY-NC-ND 4.0) License.